HIGH-ENERGY MULTIPASS FORWARD RAMAN SHIFTER AS AN EYE-SAFE LASER SOURCE FOR LIDAR

Scott M. Spuler and Shane D. Mayor

National Center for Atmospheric Research
Earth Observing Laboratory
P.O. Box 3000, Boulder, Colorado, 80307-3000, USA

ABSTRACT

A methane Raman cell optimized for generating high energy laser pulses at 1.54 microns wavelength is characterized. 1^{st} Stokes conversion efficiencies up to 43% – equivalent to 62% photon conversion efficiency – were measured. Experimental results show output average power in excess of 17.5 W, pulse energies of 350 mJ at 50Hz, with good beam quality ($M^2 < 6$.) Narrow bandwidth output is produced when pumping with a single longitudinal mode Nd:YAG laser and seeding the Stokes process with a narrowband laser diode.

1. INTRODUCTION

The nonlinear process of Stimulated Raman scattering (SRS) represents a useful and simple approach to the generation of intense, frequency-shifted radiation. Briefly described, Raman scattering occurs when a photon is inelastically scattered from a molecule leaving the molecule in an excited state and the photon wavelength shifted. If the intensity of the incident beam is very high, the initially scattered photons can further enhance the process and lead to stimulated scattering.

Raman shifting 1064 nm light from a Nd:YAG laser to 1543 nm in methane gas is an efficient means of generating high energy laser pulses in the region with the highest possible eye-safety[1; 2]. Unfortunately, early high-energy methane Raman shifters required frequent optics cleaning, and provided poor beam quality and limited pulse repetition frequency (PRF). Although many these practical limitations have been addressed, this now outdated idea of the troublesome methane Raman shifter persists in the lidar community[3].

2. DESIGN CONSIDERATIONS

Historically, for efficient stimulated Raman scattering in methane, high-energy lasers were tightly focused inside pressurized cells[4]. The high energy density from these focused-geometry cells often led to laser-induced breakdown, which was shown to be a factor limiting the conversion efficiency and the quality of the Stokes beams.[5] Furthermore optical breakdown of methane led to soot deposits, potentially damaging the Raman cell optics, and required frequent cleaning.[6; 7; 8] Experiments have shown H_2:CH_4 mixtures have higher photochemical stability compared with to pure methane [9]; however, soot formation is most effectively eliminated by reducing the energy density of the pump beam. Efficient SRS conversion with reduced pump intensity is possible by increasing the path length in a folded cell geometry.[10; 1] This approach greatly improves the reliability of CH_4 Raman shifters making them suitable for long term operation.

An additional past problem in high-energy methane Raman cells are the reactions between the gas and the anti-reflection coatings of cell windows. The inner faces of the cell windows were often etched at the exact location of the laser spot. This effect has been attributed to the laser-induced generation of reactive radicals.[5] A simple solution to this problem is to use cell windows with no coatings,[9] while a more elegant approach with higher throughput utilizes uncoated windows at Brewster's angle.[8] For our multipass design, retro-reflecting prisms were designed with a Brewster angle interface. The absence of all coatings further increases the Raman shifter durability as they are often prone to optical damage.

The limitation of higher PRF with methane Raman shifters is the local heating effect. It has been shown that without gas circulation, there is considerable optical distortion in the beam path which degrades Raman conversion efficiency.[6] The cell described herein employs a simple yet effective method to circulate the methane. Internal circulation is provided by an array of low-cost axial fans. The cell mechanical design includes internal shrouding and flow straighteners so the gas flow is laminar (minimize index changes from turbulence) and transverse to the beam plane (minimize the distance the heated gas must travel before the next laser pulse).

Without an external Stokes seed, the SRS field is initiated by spontaneously emitted photons. This stochastic process causes the energy and spatial characteristics of the output beam to fluctuate. Seeding of Raman amplifiers serves to stabilize the Stokes output[11]. Prior experiments utilizing a Stokes seed in a methane Raman cell resulted in improved conversion efficiency, especially at

lower gas pressures.[1] Those tests were performed with a broadband Nd:YAG pump laser and Stokes seeding with a narrowband distributed feedback (DFB) cw laser. Further tests were conducted for this paper including experiments using a narrowband Nd:YAG pump laser.

3. EXPERIMENTAL RESULTS

3.1. Optimization of Stokes conversion efficiency and beam quality at 10Hz

The experimental arrangement used a pump beam from a 10-Hz Q-switched Nd:YAG laser (Continuum Surelite III) at 1064 nm with a pulse width of 6 ns. An optical isolator was used to protect the laser from back-scattered light. Following the isolator, the pump beam was linearly polarized with about 615 mJ per pulse. The experimental layout is shown in figure 1. The 1st Stokes SRS process was seeded with a continuous-wave (telecommunication c-band) DFB laser. The Stokes seed beam was matched to the pump laser input diameter and overlapped in space as well as wavelength matched to Stokes centerline. The Stokes output from the Raman cell was isolated from the residual pump and any four-wave mixing (FWM) using a combination of a dichroic mirror and high dispersion Pellin Broca prism.

The initial pump beam diameter of 9 mm was reduced with a lens set as explained in Mayor and Spuler[1]. For this work a range of lens sets was explored to determine the influence of different pump beam geometries (i.e., slight convergence, divergence and entrance beam diameter) on the SRS conversion efficiency. It was found that roughly matching the fluence at the input and output of the cell produced the highest conversion efficiency. As the pump beam was heavily depleted, this required a slightly converging beam to maintain the same fluence throughout the cell. The optimal fluence was estimated at about 1.7 J/cm^2 assuming a Gaussian intensity profile. The true profile and variations (e.g., hot-spots) were not accounted for in this estimate. The optimal lens arrangement placed the theoretical pump beam waist radius (1 mm) approximately 2 meters from the exit of the cell. The Stokes output had an M^2 of 11, while achieving conversion efficiencies of up to 37% at pressures from 8.2 to 13 atm. The quantum or photon conversion efficiency in this case would be 54% since one 1064-nm photon is annihilated to create another at 1543 nm.

To improve the Stokes beam quality Argon gas was mixed with methane as a buffer gas.[12; 9] The buffer gas increases the wave-vector mismatch thereby decreasing the FWM efficiency. At active gas pressures of 6-7 atm and buffer gas pressures of 5-6 atm the Stokes beam quality was measured as an M^2 of 7. At these reduced pressures there was a slight (about 5%) reduction in conversion efficiency from the peak. However, there was a strong dependence on Stokes seeding to maintain conversion efficiency and suppress FWM. When the Stokes seed was

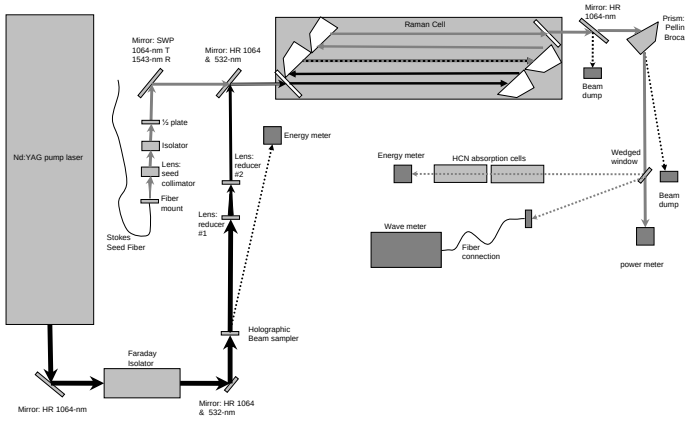

Figure 1. Experimental layout.

blocked the pump beam fluence increased (due to the slightly converging beam and reduced conversion), which damaged optical components of the cell and downstream optics. As a compromise of reliability, beam quality, and conversion efficiency, a mixture of 9.5 and 4.1 atm partial pressures of CH_4 and Ar; respectively was selected. This mixture produced a Stokes conversion efficiency of 35% with an M^2 = 9 beam quality parameter.

Following these optimization tests the Raman shifter was installed as part of a eye-safe lidar system for a field operation over a four week period. The cell, pumped with the Nd:YAG laser described above was operated for over 100 hours. At the end of the experiment the optics were carefully examined and showed no trace of contamination or damage. Furthermore, the Raman shifter was able to maintain the stringent pointing stability requirements ($<$100 μrad) of the lidar instrumentation throughout the entire project without re-alignment.[13]

3.2. Conversion efficiency and beam quality at higher PRF using narrowband Nd:YAG pump

In the next phase of the experiment, the pump laser was replaced with a 50-Hz Q-switched Nd:YAG laser (Continuum Powerlite 9050) with a pulse width of 9 ns. The laser is injection-seeded for single-longitudinal-mode operation whereas the pump in the previous experiment did not have any line-narrowing mechanism. According to the manufacturer specifications the laser has a 90 MHz bandwidth when seeded. Following the isolator, the pump beam was linearly polarized with about 905 mJ per pulse.

Stokes conversion efficiencies and beam quality were measured pumping the cell at PRFs ranging from 10 to 50 Hz. Stokes pulse energies of up to 390 mJ/pulse were measured with a 6 ns duration. Conversion efficiencies of 43% to 38% were measured from 10 to 50 Hz; respectively. The beam quality, M^2 parameter, was less than 6 at all PRFs. The results are shown in figure 2. As a note, the

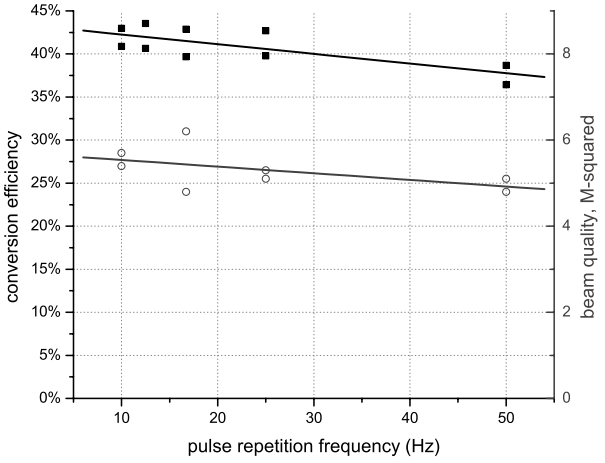

Figure 2. Experimental results of conversion efficiency (solid squares) and beam quality (open circles) as a function of pulse repetition frequency.

pump beam convergence was increased at higher repetition rates to maintain high conversion efficiencies. This was likely due to increased thermal lensing at the higher pulse rates. For all PRFs the beam convergence was set just below the threshold where backward SRS was detected.

3.3. Stokes linewidth using narrowband pump laser

For a pump wavelength of 1064 nm, the full-width half maximum (FWHM) Raman linewidth, $\Delta\nu_S$, in methane can be calculated according to following empirical formula given in[14]

$$\Delta\nu_S(p) = 8.7 + 0.39p \quad [GHz] \tag{1}$$

where p is the methane pressure in atmospheres. Eq. (1) predicts a Raman linewidth of 12.7 GHz at a pressure of 10.2 atm.

As discussed in the literature[15; 16] when the laser bandwidth is much smaller than the Raman linewidth, and when the gain is high, line narrowing occurs by amplifying the center part of the Stokes line more strongly than the wings. The gain narrowed Stokes linewidth is given by [17]

$$\Delta\nu_{S,gn}(p) = \Delta\nu_S(p)\sqrt{\ln(2)/\ln(E_f/E_i)} \tag{2}$$

where E_i and E_f are the initial and final Stokes energy. Assuming an initial Stokes energy equal to one spontaneously emitted photon ($E_i = h\ c/\lambda_S$), and the final Stokes energy of $\sim$ 300 mJ, Eq. (2) predicts a gain narrowed linewidth of approximately 1.6 GHz FWHM.

A Fizeau interferometer-based wavelength and linewidth meter (High Finesse WS-7 IR) was used to measure the spectral properties reported. As shown in the experimental layout, Fig. (1), a small fraction of the Stokes beam was picked off with a wedged window and focused onto a multi or single mode fiber which was connected to the interferometer. Without Stokes seeding the output Stokes beam had a bandwidth of approximately 1.3 GHz (10.0 pm) which is in reasonable agreement of the expected gain narrowed linewidth. With $\sim$5 mW of Stokes seeding at 1543.817 nm and pumping at 1064.500 nm, the Stokes linewidth was measured to be 210$\pm$34 MHz (1.67$\pm$0.27pm) with a center wavelength 1543.807 nm. This apparent line narrowing when Stokes seeding the SRS process is not fully understood at this time.

In the final phase of testing, the Stokes output of the Raman cell was tuned over a molecular absorption feature by adjusting the Stokes seed wavelength. As shown in Fig. (1) a small fraction of the beam was passed through two, 10 cm length, $H^{13}CN$ absorption cells. The pressure in the cells was 25 Torr and the experiment targeted the P(2) line, which has a center wavelength of 1543.8094 nm. At this pressure the linewidth of the feature is about 1.5 GHz FWHM. The Stokes linewidth, center wavelength, and pulse energy, and Stokes seed and Nd:YAG seed wavelength were measured for a one minute average for each point across the scan. The result is shown as figure 3.

To create a reference curve, the DFB seed laser (bandwidth $<$10 MHz) was tuned over the absorption feature. This is shown in Fig. 3 as a line and open circles. The Stokes output, shown as filled squares in the figure, was obtained by tuning the Stokes seed. However, it was noted that if the energy difference between the Stokes seed and pump wavelength was greater than $\pm$100 MHz (0.80 pm) from the Raman shift wavelength of 3428.61 nm the points no longer followed the reference curve.[1] Therefore, the pump wavelength was also tuned at discrete intervals by adjusting the Nd:YAG seeder wavelength. The bandwidth of the Stokes output, measured with the Fizeau interferometer, over the entire scan range from 1543.796 to 1543.866 nm, was 192$\pm$69 MHz (1.53$\pm$0.55pm).

4. CONCLUSIONS

This paper describes the optimization and characterization of a Raman shifter designed for high pulse energy applications. Experimental tests show that conversion efficiencies of $\sim$40% are obtained with good beam quality at PRFs up to 50 Hz. Initial tests show the output Stokes pulses have narrow linewidth and some tunability. For future work, we intend to implement the above transmitter to achieve long range and fast atmospheric scans. We also intend to explore the potential of aerosol backscatter calibration at 1.5 microns wavelength. If the linewidth is

[1]For clarification, the energy is described as a function of wavelength as 1/1064nm (pump)-1/3428nm(Raman shift) = 1/1543nm (Stokes output)

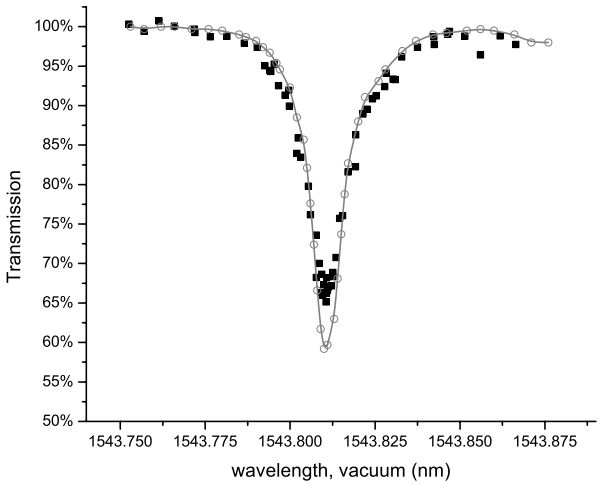

Figure 3. Experimental transmission measured tuning the Stokes output of the Raman cell over the $H^{13}CN$ P(2) line (squares). A reference curve (open circles and line) was measured by scanning feature with a DFB laser.

indeed narrow and stable, and a suitable device for use in the receiver can be created to produce equally narrow but complete absorption, it would be possible to separate molecular from aerosol backscatter.

ACKNOWLEDGMENTS

The development of the Raman cell was funded by the 2002 NCAR Director's Opportunity fund and the Earth Observing Laboratory. We would like to thank Tomas Avilez for assistance with laboratory testing and Karl Schwenz for the mechanical design of the Raman cell.

REFERENCES

1. Mayor, S. D. and Spuler, S. M. Raman-shifted eye-safe aerosol lidar. *Appl. Optics*, 43:3915–3924, 2004.
2. Spuler, S. M. and Mayor, S. Scanning eye-safe elastic backscatter lidar at 1.54 microns. *J. Atmos. Ocean. Technol.*, 22:696–703, 2005.
3. Kovalev, V. A. and Eichinger, W. E. *Elastic lidar*. John Wiley and Sons, New Jersey, 2004.
4. Brink, D. J., Burger, H. P., de Kock, T. N., Strauss, J. A., and Preussler, D. R. Importance of focusing geometry with stimulated raman scattering of nd:yag laser light in methane. *J. Phys. D Appl. Phys.*, 19:1421–1427, 1986.
5. deSchoulepnikoff, L., Mitev, V., Simeonov, V., Calpini, B., and van den Bergh, H. Experimental investigation of high-power single pass raman shifters in the ultraviolet with nd:yag and krf lasers. *Appl. Optics*, 36:5026–5042, 1997.
6. Stultz, R., Nieuwsma, D. E., and Gregor, E. Eyesafe high pulse rate laser progress at hughes. In *Eyesafe Lasers: Componets, Systems, and Applications*, volume 1419, pages 64–74. SPIE, 1991.
7. Spinhirne, J. D., Chudamani, S., Cavanaugh, J. F., and Bufton, J. L. Aerosol and cloud backscatter at 1.06, 1.54 and 0.53 microns by airborne hard-target-calibrated nd:yag/methane raman lidar. *Appl. Optics*, 36:3475–3490, 1997.
8. Shaw, M. J., Partanen, J. P., Owadano, Y., Ross, I. N., Hodgson, E., Edwards, C. B., and O'Neill, F. High-power forward raman amplifiers employing low-pressure gases in light guides. ii. experiments. *J. Opt. Soc. Am. B*, 3(10):1466 – 1475, 1986.
9. Simeonov, V., Mitev, V., van de Bergh, H., and Calpini, B. Raman frequency shifting in a ch_4:h_2:ar mixture pumped by the fourth harmonic of a nd:yag laser. *Appl. Optics*, 37:7112–7115, 1998.
10. Kurnit, N. A., Harrison, R. F., Karl-Jr., R. R., Brucker, J. P., Busse, J., Grace, W. K., Peterson, O. G., Baird, W., and Hungate, W. S. Generation of 1.54 micron radiation with application to an eye-safe laser lidar. In Press, S., editor, *Proceedings of the International Conference on LASERS '97*, pages 608–610, McLean, VA, 1998.
11. Wessell, J. G., Repasky, K., and Carlsten, L. J. Competition bewteen spontaneous scattering and stimulated scattering in an injection-seeded raman amplifier. *Physical Review A*, 53:1854–1860, 1996.
12. Schoulepnikoff, L. and Mitev, V. High-gain single pass stimulated raman scattering and four-wave mixing in a focused beam geometry: a numerical study. *Pure Applied Optics*, 6:277–302, 1997.
13. Mayor, S. D., Spuler, S. M., and Morley, B. M. Scanning eye-safe depolarization lidar at 1.54 microns and potential usefulness in bioaerosol plume detection. In *Lidar Remote Sensing for Environmental Monitoring IV*. Society of Photo-Optical Instrumentation Engineers, Society of Photo-Optical Instrumentation Engineers, 2005.
14. Kazzaz, A., Ruschin, S., Shoshan, I., and Ravnitsky, G. Stimulated raman scattering in methane - experimental optimization and numerical model. *IEEE Journal of Quantum Electronics*, 30:3017–3024, 1994.
15. Wang, C. S. Theory of raman scattering. *Physical Review*, 182(2):482–494, 1969.
16. Raymer, M. G. and Mostowski, J. Stimulated raman scattering: Unified treatment of spontaneous initiation and spatial propagation. *Physical Review A*, 24(4):1980–1992, 1981.
17. MacPherson, D. C., Swanson, R. C., and Carlsten, J. L. Quantum fluctuations in the stimulated-raman-scattering linewidth. *Physical Review Letters*, 66(1):66–69, 1988.